*Desalination and Water Treatment*
www.deswater.com

doi: 10.5004/dwt.2023.30075

313 (2023) 92–105
November

# De-emulsification performance and mechanism of polyether-polyquaternium copolymers and compounding products on tight gas produced water

Kai-wen Liu[a], Peng-cheng Hao[b], Zhi-qiang Hu[a], Xiang-wei Li[a], Fei Meng[c], Xian-zhe Guo[d,*], Zhuo-zhuang Liu[d], Wu Chen[d,*]

[a]*Jianghan Machinery Research Institute Limited Co. of CNPC, Hubei 434000, China, emails: liukaiw@cnpc.com.cn (K.-w. Liu), huzhiqiangdr@cnpc.com.cn (Z.-q. Hu), 249064050@qq.com (X.-w. Li)*
[b]*PetroChina Coalbed Methane Company Limited, Beijing 102200, China, email: haopengcheng@petrochina.com.cn (P.-c. Hao)*
[c]*PetroChina Changqing Oilfield Company, Xi'an, 710018, China, email: 56618845@qq.com (F. Meng)*
[d]*College of Chemistry and Environmental Engineering, Yangtze University, Hubei 434023, China, emails: gxz202071217@163.com (X.-z. Guo), ccww91@126.com (W. Chen)*

Received 6 June 2023; Accepted 9 October 2023

**ABSTRACT**

As the development of tight gas fields enters the stable production stage, condensate oil forms a complex oil–water emulsifying system under the action of bubble drainage agent, corrosion inhibitor, hydrate inhibitor, and other additives to increase and stabilize production, as well as the formation of particulate matter. A new demulsification and flocculation agent suitable for condensate emulsifying system is developed to make the system unstable and the oil beads coalesce. In this paper, a polyether–quaternary ammonium salt reverse demulsifier (PPA) was synthesized by grafting a cationic group onto a five-membered block polyether X-75. A new type of demulsification–flocculation agent (CQ) was obtained through the complex modification of PPA and inorganic coagulant polyaluminum ferric chloride. Fourier-transform infrared spectroscopy, X-ray photoelectron spectroscopy, and gel chromatograph were used to characterize the group and molecular structure. The reaction parameters were optimized by single-factor experiment and the response surface method, and the demulsification–flocculation mechanism was determined by zeta potential, interfacial tension, and fractal dimension. Results showed the PPA demulsifier has active groups (block polyether) and cationic groups (polyquaternary ammonium salt) at the oil–water interface at the same time and can play a synergistic role between them. Single-factor experiment and response surface optimization showed CQ concentration and temperature were key factors affecting the demulsification–flocculation effect. When CQ concentration was 547 mg/L, settling temperature was 27.9°C and PPA accounted for 71%. After settling for 30 min, the oil content and the concentration of total suspended solids (TSS) in the water decreased to 21.26 and 7.0 mg/L, respectively, which met the water quality requirements of reinjection (oil content ≤ 30 mg/L, TSS concentration ≤ 15 mg/L). By neutralizing and displacing active substances at the oil–water interface and sweeping by net trapping, CQ can coagulate oil beads and suspended particles to form large flocs and realize the efficient separation of oil beads, suspended particles, and water.

*Keywords:* Flocculation; Demulsification; Electro neutralization; Net trapping; Polyether–polyquaternium copolymer; Compounding; Tight gas produced water

* Corresponding author.

## 1. Introduction

Tight gas is an unconventional natural gas produced in low-permeability tight sandstone reservoirs and is the first unconventional natural gas resource to be exploited industrially [1]. China is rich in tight gas resources, with proven reserves reaching $4 \times 10^{12}$ $m^3$ and tight gas production accounting for 70.1% of the total unconventional gas production in 2018, which has become one of the important energy replacement types for conventional natural gas [2]. Several tight gas fields, represented by Surig and Daniudi in the Ordos Basin and Sujiahe in the western Sichuan Basin, have been placed into large-scale development, driving the rapid development of tight gas in China [3,4].

During tight gas extraction, a large amount of tight gas produced water (TPW) is generated due to the return of fracturing fluid and the intrusion of formation water. An estimated $5.70 \times 10^8$ $m^3$ of TPW is produced annually in the United States due to unconventional gas extraction [1,5], and the average water content of a horizontal well in an area of the Daniudi gas field in China is 5.65 $m^3$/d, with an average water-to-gas ratio of 6.5 $m^3/10^4$ $m^3$ [4]. Therefore, TPW accounts for the largest volume of byproducts in tight gas extraction [6], and its composition depends on the structure of fracturing fluid and formation water and the reservoir properties [7]. The composition of TPW is complex, depends on the structure of fracturing fluid and formation water and the nature of gas reservoir, and is characterized by complex composition, highly variable main water quality monitoring indicators in time and space, high mineralization, and generally high suspended matter content and chemical oxygen demand [7–9]. In addition, the extraction of many domestic and foreign natural gas reservoirs is accompanied by a certain amount of liquid oil, called condensate, which is caused by the reduction of reservoir pressure to below the dew point pressure [10]. As the gas field development enters the stable production stage, various production enhancement agents, such as foam drainage agents, corrosion inhibitors, hydrate inhibitors, and other agents are used to ensure the recovery of natural gas, thus making the polymeric organic matter in TPW gradually increase, while the condensate may be emulsified under the action of various production enhancement and stabilization agents and particulate matter formation [11,12]. Together with the strong shear and gas–liquid velocity difference generated at the mechanical throttle, bend, and valve leading to the strong mixing of water and oil, TPW forms a stable oil-in-water (O/W) emulsion system, which is one of the most challenging industrial wastewater at present, thus necessitating the search for economically efficient treatment solutions for the sustainable development of this fast-growing unconventional energy source.

Conventional methods for treating TPW include single or combined methods such as demulsification, coagulation/flocculation, dissolved air flotation, membrane separation, biological treatment, and oxidation [13,14]. Chemical demulsification, which is suitable for the treatment of large volume of produced water and has the advantages of simple operation, great treatment effect, and low cost, is a common wastewater treatment in the oil and gas field industry and is often used as a pretreatment for emulsified oil in TPW to reduce the difficulty of subsequent treatment [15]. Studies have shown O/W emulsions are stabilized by the double-layer repulsion between droplets, whereas reverse demulsifiers are a class of water-soluble demulsifiers that can effectively neutralize the negative charge on the surface of droplets in O/W emulsions, thus promoting flocculation and agglomeration of oil droplets [16,17]. Common reverse demulsification include polyquaternium, polyether–polyquaternium copolymer (PPA), polyacrylates, ethylene oxide–propylene oxide polyether block copolymer, dendrimers, and other types [18–20]. In comparison, PPA can bring into play the strong affinity, low surface tension, and high chemical stability of polyether demulsification for oil–water interfacial films and the excellent electrical neutralization performance of quaternary ammonium cationic demulsification, thus further improving the reverse demulsification efficiency [21]. Duan et al. [22] prepared a new reverse demulsifier (PDMP) by copolymerizing block polyether macromonomer (PEP-65) and dimethyl diallyl ammonium chloride, and the oil removal effect of PDMP on O/W emulsion was more than three times that of commercial reverse demulsifiers. Compared with poly(dimethyl diallyl ammonium chloride) (PDADMAC) synthesized under the same conditions, the oil–water interfacial partition coefficients of PDMP were higher than those of PDADMAC at different water–oil ratios, which was attributed to the presence of hydrophobic PEP-65 graft in PDMP, resulting in better amphiphilicity of PDMP than PDADMAC and better interfacial activity. Sun et al. [17] prepared demulsifier PPA for the demulsification of simulated O/W emulsions, and the oil content of the simulated extracted fluid could be reduced from 500 to 97.0 mg/L at a dosing rate of 110 mg/L, with an oil removal rate of 80.6%, which was much higher than that of 65.9% for commercial S-01 demulsification under the same conditions. This remarkable demulsification efficiency was attributed to its ability to reduce interfacial tension (IFT), decrease interfacial film thickness, reduce elastic modulus, and neutralize negative charge of interfacial film.

In addition, coagulation methods have been widely used for oily wastewater treatment and have proven to be cost effective. Inorganic salts of various high-valent metals or polymeric inorganic polymers, although with different mechanisms, compressed double layers, and charge neutralization, are usually considered the main ones that can provide similar effects as reverse demulsifiers [15,23]. Zhai et al. [24] used polymerized ferric sulfate (PFS) and polymerized aluminum chloride (PAC) for the pretreatment of produced water from a gas field in Chongqing, China (initial oil content of 37.4 mg/L) and found that under optimal conditions, the oil removal rate of PFS (98.9%) was higher than that of PAC (95.3%). Sun et al. [25] prepared a composite coagulant-polymerized ferric aluminosilicate (PAFS), which could treat high-concentration oily wastewater at 5,000 mg/L under the condition of using PAM as coagulant aid; when the dosage of PAFS was 120 mg/L, the removal rates of chemical oxygen demand (COD) and oil by PAFS were 98.2% and 98.4%, respectively. However, inorganic coagulants still have defects such as low agglomeration efficiency, high sensitivity to pH, and excessive concentration of residual metals in treated water, and the current application

is still highly restricted [15,26]. Therefore, more researchers are now focusing on the development of inorganic–organic composite agents to consider the charge neutralization, colloidal particle adsorption, and bridging effects of coagulants and the strong ability of demulsification to destroy the emulsion layer to achieve the efficient removal of suspended matter and condensate in TPW. For example, Yang et al. [27] prepared a new high-efficiency wastewater treatment agent (YL-7) by compounding demulsifier (LY), flocculant (PDMDAAC), and coagulant (PAC) at the ratio of 10:3:3 by mass concentration. The optimum experimental conditions were YL-7 dosage of 320 mg/L, settling temperature of 50°C, and settling time of 90 min. Under these conditions, the oil content of the extracted water was reduced from 728.8 to 23.7 mg/L, and the oil removal efficiency reached 96.7%. The price of the inorganic coagulant is much lower than that of the reverse demulsifier, and the use of coagulant to replace reverse demulsifier partially can also significantly reduce the treatment cost.

In this paper, a multi-branching PPA demulsifier was synthesized and compounded with an inorganic coagulant for the treatment of actual TPW, followed by the optimization of the optimal treatment conditions using response surface methodology (RSM) and the evaluation of the adaptability of the compound. Finally, the demulsification–flocculation mechanism was proposed by means of IFT, zeta potential, and fractal dimension. The aim of this paper is to develop an efficient, low-cost compound PPA demulsifier to provide a technical basis for the pretreatment of oil-bearing produced water from gas fields.

## 2. Materials and methods

### 2.1. TPW sample

The characteristics of TPW vary by well location and completion practice [28]. In this paper, the TPW sample was obtained from a three-phase separator at the Number 3 Gas Production Plant, Changqing Gas Field, Inner Mongolia Autonomous Region (China). The collected gas wells had been operated for more than 1 y. The water samples were stored in the laboratory at room temperature, and the experiments were completed within about three months to avoid significant changes in the properties of the samples during storage. Table 1 lists the water quality indicators of TPW.

### 2.2. Chemicals

The five-membered block polyether X-75 was synthesized by our group based on the previous research. Polyaluminum ferric chloride (PAFC) was purchased from Henan Shiyuan Water Purification One-stop Service Center, China. Phosphorus tribromide (99%), chloroform (AR), N,N-dimethyldodecylamine, and other drugs were purchased from Shanghai Maclean Biochemical Technology Co. All reagents were used directly without further purification treatment.

### 2.3. Synthesis of PPA and CQ

First, 10.0 g of the five-membered block polyether demulsifier X-75 was placed in 100 mL of chloroform, and 50 mL of phosphorus tribromide in chloroform solution (10 mol/L) was added dropwise at 5°C in a water bath. Next, the reaction temperature was gradually increased to 60°C, and the reaction was refluxed for 150 min. After the reaction system was cooled to room temperature, 50 mL of aqueous sodium hydroxide solution with a concentration of 30 mol/L was added and left to stratify, the lower layer was separated and dried with anhydrous sodium sulfate, and the solvent was evaporated under reduced pressure to 2 kPa. The product was then reacted with 0.5 mol of dodecyl dimethyl tertiary amine in 100 mL of anhydrous ethanol in an oil bath at 80°C for 4 d, and the solvent was evaporated under reduced pressure to obtain polyether–polyquaternium copolymer PPA.

Next, the prepared PPA demulsifier was dissolved in water with PAFC, and the compound demulsifier CQ was prepared by heating and stirring in a water bath at 50°C for 1 h. The ratios (w/w) of PPA and PAFC were adjusted to 5:0, 4:1, 3:2, 1:1, 2:3, and 1:4, and the resulting products were expressed as CQ (100%), CQ (80%), CQ (60%), CQ (50%), CQ (40%), and CQ (20%), respectively.

### 2.4. Characterization

The prepared PPA demulsifier was characterized: The samples were ground together with KBr and pressed into thin flakes in a mold, and the functional groups of the materials were characterized by Fourier-transform infrared spectrophotometer (FTIR, Nicolet 6700, Thermo Fisher, USA) in the wave number range of 500–4,000 $cm^{-1}$. The surface chemical composition and valence of PPA were characterized by X-ray photoelectron spectrometer (XPS, K-Alpha, Thermo Fisher, USA), the data were analyzed by Avantage software, and the peaks were calibrated at the C1s adsorption carbon C–C energy position of 284.8 eV. The relative molecular masses of the samples and their distributions were determined by gel permeation chromatography (PL-GPC-50,

Table 1
Physiochemical characteristics of produced water

| Parameter | Value |
|---|---|
| pH | 6.15 |
| Total suspended solids (TSS), mg/L | 185.5 |
| Total dissolved solids (TDS), mg/L | 38,327.58 |
| Chemical oxygen demand (COD), mg/L | 7,362.02 |
| Total organic carbon (TOC), mg/L | 1,150.03 |
| Oil content, mg/L | 72.63 |
| Chromaticity, Times | 256 |
| Turbidity, NTU | 157.82 |
| $K^+$, mg/L | 233.25 |
| $Na^+$, mg/L | 6,805.76 |
| $Ca^{2+}$, mg/L | 6,747.87 |
| $Mg^{2+}$, mg/L | 593.16 |
| $Cl^-$, mg/L | 23,469.76 |
| $SO_4^{2-}$, mg/L | 2.01 |
| $HCO_3^-$, mg/L | 826.09 |
| $Fe^{3+}$, mg/L | 3.58 |

Polymer, UK), equipped with two columns, namely, Sho-dexA803 and Sho-dexA805, with a relative molecular mass range of 580–7,500 Da, using a differential detector, with monodisperse. The measurement temperature was 35°C, and ultrapure water was used as the mobile phase with a flow rate of 1.0 mL/min.

The oil droplet size distribution of the TPW samples before and after breakage was determined using a digital microscope (DMS1000, Leica, Germany), the zeta potential of the dispersed oil droplets was determined by a Malvern laser particle size meter (Nano ZS, Mastersizer Micro, UK), and the oil–water IFT was measured by an IFT meter (K100, KRÜSS, Germany) and calculated by Eq. (1). The flocs generated during flocculation were captured using a floc morphology analyzer (R-V1.0HIT, China), those with good imaging effect were selected and analyzed by image analysis software, and the fractal dimension of the generated flocs was calculated by Eq. (2).

$$F = \gamma \cdot D \tag{1}$$

$$\ln A = D_f \ln P + \ln \alpha \tag{2}$$

where $\gamma$ (mN/m) is the IFT, $D$ (m) is the perimeter of the working platinum sheet, $F$ (mN) is the separation force, $A$ is the projected area of the floc particles, $P$ is the projected perimeter, $\alpha$ is the proportionality constant, and $D_f$ is the fractal dimension of the floc in two dimensions.

### 2.5. Reverse demulsification tests

The demulsification–flocculation experiments were conducted in 500 mL beakers, and the 500 mL water samples were preheated in a constant-temperature water bath for 30 min before the start of the experiments. Next, a predetermined amount of PPA demulsifier or compound demulsifier was added to the TPW wastewater. The samples were stirred with a hexagonal stirrer at an initial fast speed of 400 rpm for 45 s to disperse the agents uniformly, stirred slowly at 50 rpm for 5 min, and then left for 25 min. Subsequently, the supernatant was collected from a depth of 3 cm below the water surface and used to measure residual oil concentration and turbidity. The effects of agent dosage, compounding ratio, temperature, and settling time on the effectiveness of TPW were investigated by controlling individual variables. All experiments were repeated two to three times to determine the average value.

The oil content in TPW before and after treatment was determined by taking a certain volume of TPW into a partition funnel, adding HCl (1:1) to adjust the pH of the wastewater to <2, followed by adding petroleum ether (boiling range 30°C–60°C) several times and shaking thoroughly, combining the organic phases and drying with anhydrous $Na_2SO_4$, followed by measuring the absorbance at 210 nm on a UV-Vis spectrophotometer (TU-1900, China). Turbidity was evaluated according to China national standard GB/T 13200-199 "Water Quality - Determination of Turbidity", and oil content and the rates of change of turbidity before and after treatment were calculated by Eqs. (3) and (4), respectively.

$$C = \frac{E \cdot V_0}{K \cdot V_w} \tag{3}$$

$$R(\%) = \frac{A_0 - A_1}{A_0} \times 100\% \tag{4}$$

where $C$ is the oil content (mg/L); $E$ is the absorbance of the measured water sample; $K$ is the absorbance coefficient (L/mg); $V_W$ and $V_O$ represent the volume of water sample and petroleum ether, respectively; $R$ (%) is the removal rate of turbidity; $A_0$ and $A_1$ represent the turbidity of TPW before and after treatment, respectively.

### 2.6. Response surface method optimization experiment

The optimal response surface optimization of the demulsification–flocculation conditions was based on the Box–Behnken central combination design principle [29]. Based on the results of the single-factor experiments, PPA percentage, temperature, and CQ concentration were selected as the three factors, and the three optimal levels initially derived from the single-factor experiments were chosen. The experiments were carried out according to software Design–Expert 12 design scheme, the model was fitted to the experimental data using a quadratic polynomial fitted by the least squares method, the fitted model was subjected to analysis of variance and significance test, and response surface analysis was performed on the fitted model to derive the theoretically optimal parameter combinations, which were verified by indoor experiments.

## 3. Results and discussion

### 3.1. Characterization of TPW

Table 1 shows the produced water is close to neutral, and the oil content and total suspended solids (TSS) content in the water are 72.63 and 185.5 mg/L, respectively, which are much higher than the relevant standards (China) for reinjection or internal reuse. The high COD and total organic carbon (TOC) of TPW indicate its dissolved organic is remarkably high, which makes realizing reuse or external discharge more difficult. The total dissolved solids (TDS) content of TPW is as high as 38,327.58 mg/L, which may be due to the dissolution of highly mineralized brine and initially injected fracturing fluid in the underground shale formation; $Cl^-$, $Na^+$, and $Ca^{2+}$ are the most abundant anions and cations in the water; the water quality is of $CaCl_2$ type, which may lead to serious corrosion of the gas field water treatment system [7,30]. Finally, the zeta potential of TPW is −7.152 mV, indicating the oil beads in TPW are negatively charged, suggesting the wastewater is mainly O/W emulsified wastewater [17,23].

### 3.2. Characterization of PPA

The functional groups of the synthesized PPA demulsification were characterized using FTIR (Fig. 1a). Strong, broad absorption peaks are at 3,421.8 $cm^{-1}$, which are attributed to the stretching vibration of O–H or N–H, whereas that at 1,632.9 $cm^{-1}$ corresponds to the deformation vibration of O–H or N–H [31]. Distinct bands are near 1078.4 and 983.1 $cm^{-1}$, which are attributed to C–N and C–O stretching vibrations, respectively [32]. Of particular interest is the absorption

band at 1,401.0 $cm^{-1}$, which is deemed the bending vibration of $-CH_3$ in the $-N^+(CH_3)_3$ group [33]. The above results indicate the PPA demulsifier contains characteristic groups such as hydroxyl, alkoxy, and quaternary amino groups.

The functional groups and relative contents of PPA were further analyzed by XPS. The C 1s high-resolution spectrum in Fig. 1b can be deconvoluted into three fitted peaks centered at 284.8, 286.3, and 289.0 eV, which are attributed to C–C/C=C/C–H (76.9%), C–O (20.0%), and C–O–C (3.1%), respectively [34], and the most occupied ratio of C–C/C=C/C–H bonds indicates PPA has an abundant hydrophobic structure and is easily adsorbed at the oil–water interface. For the high-resolution XPS spectrum of N 1s (Fig. 1c), PPA exhibits two fitted peaks with binding energies of 400.1 and 402.4 eV, which belong to C–N (73.5%) and $-N^+(CH_3)_3$ structures, respectively [33], confirming PPA contains more quaternary amino groups, which can effectively neutralize the negative charge on the surface of the O/W emulsion. The O 1s peaks at 531.0, 532.3, and 533.9 eV are deconvoluted into three spectral bands (Fig. 1d), representing C–O, C–O–C, and –OH, respectively [35], with relative contents of 12.8%, 67.1%, and 20.1%, respectively; the higher C–O–C structure percentage confirms the block polyether structure in the PPA species, which is consistent with the FTIR results.

The average molecular weight number (Mn) and average molecular weight (Mw) of the PPA determined by GPC are 1,241 and 1,504 Da, respectively, and the higher molecular weight demulsifier could replace the natural emulsifier at the oil–water interface more effectively to achieve the agglomeration of emulsified oil [36]. In addition, the polydispersity coefficient (i.e., the ratio of Mw to Mn) of the samples is 1.211. The smaller the polydispersity coefficient is, the narrower the molecular weight distribution of the polymer, which indicates the degree of polymerization of the synthesized PPA is similar [37].

### 3.3. Performance of PPA

The effect of the dosage of PPA on the removal of oil and suspended matter in TPW was first evaluated (Fig. 2). At low concentrations, the polymers available to adhere to the kaolin suspension particles and the electrical neutralization of the positive charges are not sufficient to destabilize the TPW [23,38]. Thus, it is less effective in removing turbidity and emulsified oil. When the PPA dosage was increased to 400 mg/L, the turbidity removal rate increased significantly, indicating the PPA agent has good flocculation and sedimentation performance; the contribution of continuing to increase the dosage to turbidity removal was not significant. The oil content in TPW decreased from 72.63 to 18.25 mg/L when the PPA dosage was 500 mg/L, which met the limit of oil content in the reinjection water quality

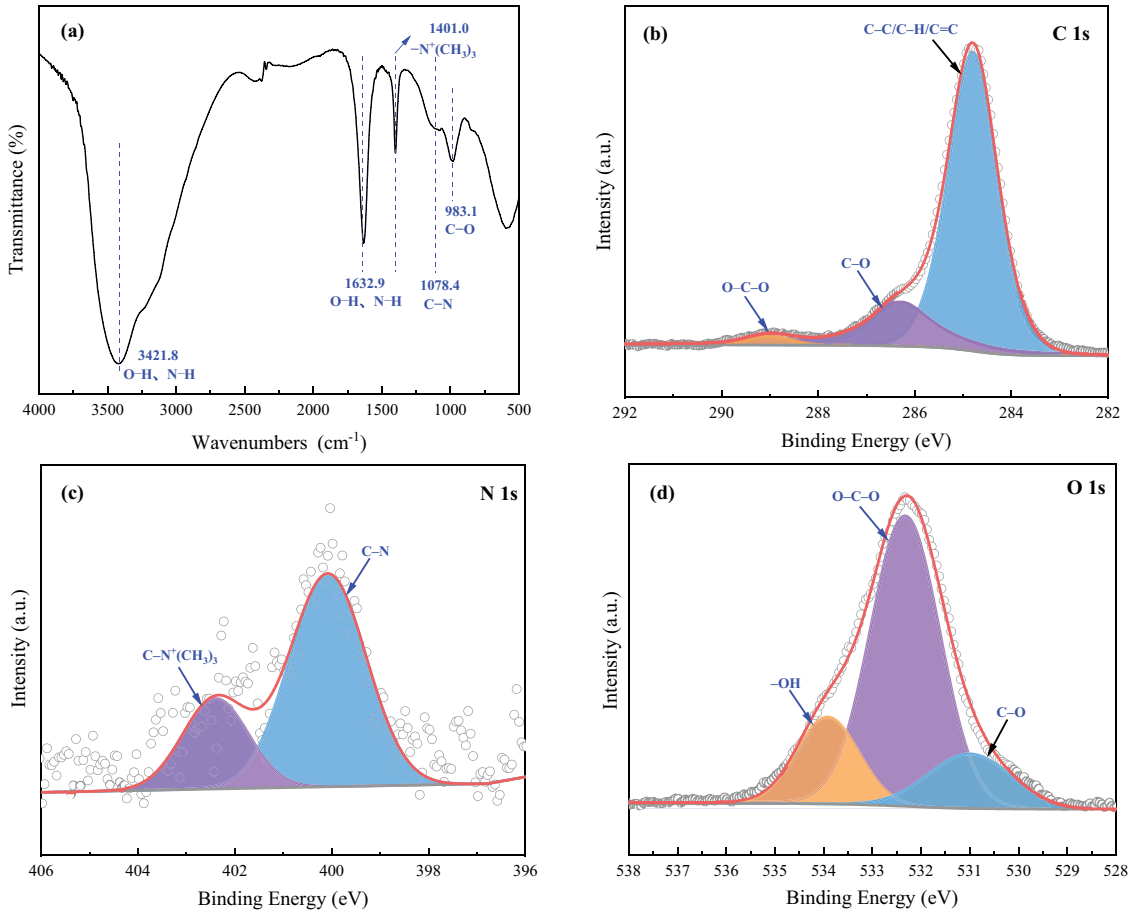


Fig. 1. (a) FTIR spectra of PPA, high-resolution XPS spectra of (b) C 1s, (c) N 1s, and (d) O 1s.

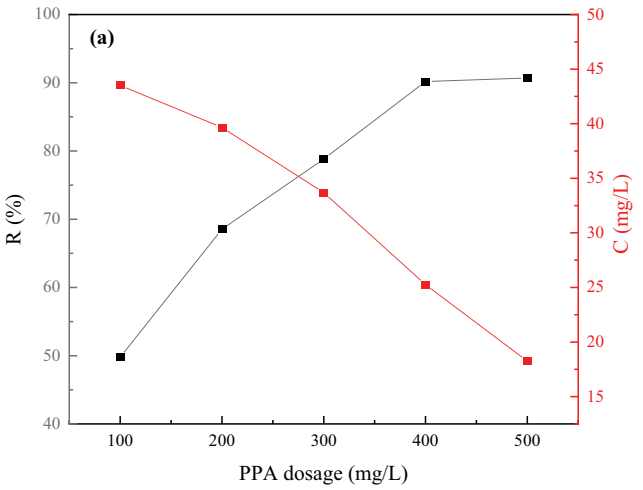


Fig. 2. Effect of PPA dosage on the demulsification–flocculation efficiency (temperature 25°C).

index of this gas field. The great demulsification–flocculation effect of PPA may be due to the presence of polyether and quaternary ammonium salt structures in its structure, and the block polyether has high surface activity and adsorbs at the oil–water interface, replacing the naturally occurring emulsifier or surfactant and weakening the interfacial film strength to promote collision and agglomeration of small oil droplets [22]. The high positive charge density of quaternary ammonium salts ensures they can neutralize the negative charge on the surface of emulsified oil droplets and destabilize the double electric layer of the dispersed phase [15]. The larger molecular weight and multibranched structure also have strong adsorption bridging or net trapping effects [17].

### 3.4. Performance and condition optimization of CQ agents

The combination of inorganic coagulant and reverse demulsifier is one of the methods to exploit the synergistic effect between them and effectively reduce the cost [39]. Therefore, the effects of modified compounding ratio, dosage, reaction temperature and settling time on the demulsification–flocculation efficiency were investigated.

#### 3.4.1. Effect of PPA ratio

Different composite CQ demulsification–flocculation processes were synthesized by changing the PPA percentage (Fig. 3a), and the removal effect of turbidity and oil content of TPW significantly worsened as the PPA percentage decreased, especially in the range of 20%–60% of PPA. Numerous minute flocs could be observed in the water after adding the agent, but agglomeration had difficulty causing sedimentation, so the turbidity increased rather than decreased compared with the initial value. In addition, the oil removal effect worsened, which may mean that PPA plays an important role in the destabilization and agglomeration of emulsified oil. Therefore, CQ (80%) was selected for further investigation in the subsequent experiments.

#### 3.4.2. Effect of CQ dosage

The treatment effects on the turbidity and oil content of TPW were investigated when the CQ dosage was varied between 200 and 600 mg/L. Fig. 3b shows the oil concentration in TPW decreased with increasing CQ dosage, which could significantly reduce the oil content in TPW to 11.75 mg/L at a CQ dosage of 600 mg/L. This outcome was because CQ neutralized the negative charge on the surface of the oil droplets and strongly topped off the interfacial film, which led to the mutual agglomeration of small oil droplets [40,41]. For turbidity, the flocs produced at low CQ doses (<400 mg/L) were difficult to flocculate and settle within 30 min, resulting in a significant increase in turbidity relative to the initial turbidity [38].

#### 3.4.3. Effect of temperature

Temperature is an important parameter in demulsification–flocculation, which affects the state of CQ agents in the wastewater and the agglomeration of water droplets [42]. Fig. 3c shows the demulsification–flocculation efficiency at different settling temperatures for CQ with a dosage of 500 mg/L. When the temperature was increased from 15°C to 35°C, the oil concentration in TPW decreased from 25.44 to 20.14 mg/L after settling for 30 min, indicating the effect of temperature on the oil removal efficiency is not significant. However, the increase in temperature significantly reduced the turbidity of TPW, and the turbidity removal rate reached 98.37% at the temperature of 35°C, which is close to 100%. This result is because the Brownian motion is significantly accelerated by increasing temperature, and the frequency of the mutual effective collision among the formed micro flocs is significantly accelerated, which is conducive to the flocculation and aggregation of the micro flocs, thus leading to the rapid settling of flocs [39,42]. An increase in temperature also reduces the viscosity of the continuous phase, which leads to a series of effects such as an increase in the settling and separation rate of the emulsion, an increase in the discharge rate of the continuous phase liquid between the oil beads and the flocs, and an increase in the aggregation rate of the oil beads [41,43]. Considering the effect and energy saving, 30°C was chosen as the best demulsification–flocculation temperature.

#### 3.4.4. Effect of settling time

After the addition of CQ agent, settling is needed to separate oil and suspended matter from water. Fig. 3d shows the effect of settling time on the demulsification–flocculation efficiency. The oil and turbidity removal efficiency increased significantly with the increase of settling time, but almost no change occurred after 30 min. This result is because after the addition of CQ agent, the PPA molecules in it first adsorbed on the oil–water interface, which combined small oil droplets with large oil droplets through demulsification and charge neutralization. Then, the oil droplets and suspended matter attached to the floc formed by PAFC, and the agglomerative growth and settling of the floc took some time; therefore, the settling time of 30 min was deemed appropriate in this paper [23,27].

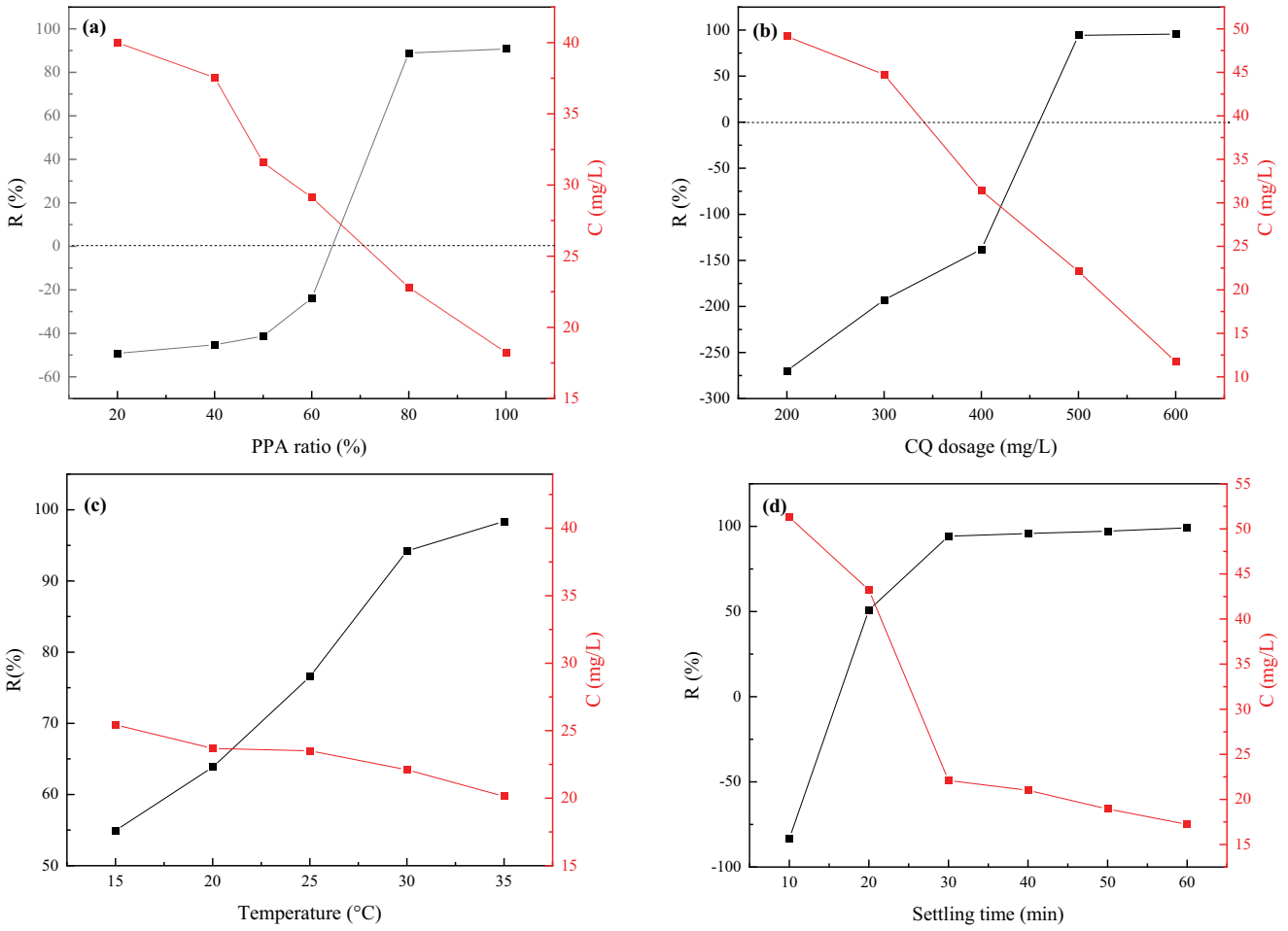


Fig. 3. Effects of (a) PPA ratio, (b) CQ dosage, (c) temperature, and (d) settling time on demulsification–flocculation efficiency (dosage 500 mg/L, temperature 30°C, and settlement time 30 min).

### 3.5. Response surface method optimization and analysis of results

#### 3.5.1. Establishment and analysis of regression model

To investigate the best combination of test conditions for CQ on the demulsification–flocculation stage of TPW and to enhance the scientific and rational nature of the test, a three-factor, three-level response surface experiment was conducted using Box–Behnken of Design Expert 12 on the percentage of PPA, settling temperature, and CQ concentration in demulsification–flocculation. The oil content in TPW ($Y$) after 30 min of settling was used as the index. Tables 1 and 2 show the experimental design and response values, respectively.

The least squares regression analysis was performed using Design–Expert 12 for each factor level and response value of the BBD design (Table 3), and the regression is shown in Eq. (5). The regression equation shows the coefficients of the quadratic effects are all positive, indicating the parabolic opening of the quadratic regression equation is upward and the equation has a minimum value, that is, the test can be optimized by BBD response surface optimization analysis to obtain the optimal solution [44].

Table 2
Experimental factors and levels

| Factors | Code | Levels | | |
|---|---|---|---|---|
| | | –1 | 0 | 1 |
| CQ concentration (mg/L) | $A$ | 400 | 500 | 600 |
| PPA ratio (%) | $B$ | 60 | 80 | 100 |
| Temperature (°C) | $C$ | 20 | 25 | 30 |

$$Y = 298.1 - 3.839C - 426.3B - 0.2622A + 0.0930C^2 + 375.5B^2 + 0.000279A^2 - 2.204BC + 0.000378AC - 0.0759AB \quad (5)$$

#### 3.5.2. Model variance analysis and significance test

Table 4 shows the results of the significance and ANOVA analysis. The regression model $P < 0.0001$, which indicates the fitted regression model is significant and the prediction model can explain the variability of the experimental data well [29]. The misfit term of the model $P = 0.2167 > 0.05$

and not significant; the coefficient of determination of the model $R^2$ = 0.9927, $R_{Adj}^2$–$R_{Pred}^2$ = 0.9797–0.8989 = 0.0808 < 0.2, indicating the regression equation model is credible, can be fitted well with the experimental data, and can be used to analyze and predict the oil removal performance of CQ demulsification–flocculation [45,46].

### 3.5.3. Response surface analysis

The response surface plot is a 3D surface plot of the response value to each factor, which can visually reflect the interaction between factors [47]. Fig. 4 shows the interaction and influence between the factors can be represented by the steepness of the curve trend in the response surface and the density of contour lines in the contour plot [48,49]. Fig. 4a–c show the response surfaces of temperature and CQ dosage are steeper and the contour lines are denser, whereas the response surface of PPA percentage is smooth and the contour lines are the most sparse, which verifies that the influence on oil content after demulsification is ranked as $A > C > B$, that is, CQ dosage > temperature > PPA percentage, which is consistent with the data in Table 4 and Fig. 5. In addition, the oil content after demulsification decreases with the increase of temperature and starts to increase after reaching the lowest center point when the temperature is close to 28°C. The amount of demulsification and the proportion of PPA have the same trend, and the oil content in water is the lowest at 550 mg/L and about 80%, respectively. In summary, the values of each factor need to be optimized to make the best parameters of the demulsification–flocculation.

Table 3
Experimental design and response values

| No. | *A* | *B* | *C* | *Y* (mg/L) |
|---|---|---|---|---|
| 1 | 500 | 60 | 20 | 31.28 |
| 2 | 500 | 60 | 30 | 27.70 |
| 3 | 500 | 100 | 20 | 35.14 |
| 4 | 500 | 100 | 30 | 27.16 |
| 5 | 400 | 80 | 20 | 34.42 |
| 6 | 400 | 80 | 30 | 29.07 |
| 7 | 600 | 80 | 20 | 29.26 |
| 8 | 600 | 80 | 30 | 24.67 |
| 9 | 400 | 60 | 25 | 32.56 |
| 10 | 400 | 100 | 25 | 34.98 |
| 11 | 600 | 60 | 25 | 28.11 |
| 12 | 600 | 100 | 25 | 27.49 |
| 13 | 500 | 80 | 25 | 24.60 |
| 14 | 500 | 80 | 25 | 23.91 |
| 15 | 500 | 80 | 25 | 24.21 |

### 3.5.4. Analysis of the results of the validation experiment

Using Design-Expert, the above three factors were optimized to minimize the oil content in the treated water. According to the prediction, the oil content in TPW can be reduced to 22.85 mg/L when the CQ addition is 547.5 mg/L, the PPA percentage is 70.5%, and the settling temperature is 27.88°C. Based on the predicted conditions, the optimal process conditions were adjusted to the temperature of 27.9°C, the PPA percentage of 71%, and the CQ dosage of 547 mg/L. The oil content after treatment was then obtained as 21.26 mg/L, which was 6.96% different from the predicted value, indicating the model prediction was accurate and credible.

Table 5 compares the main water quality indicators of TPW before and after treatment under these conditions. The TSS and oil content in TPW decreased significantly after the demulsification–flocculation to 21.26 and 7.0 mg/L, respectively, which met the water quality requirements of the reinjection wells in the Changqing gas field. In addition,

Table 4
Significance testing of regression model coefficients and analysis of model variance

| Source | Sum of squares | df | Mean square | *F*-value | *P*-value | Significance |
|---|---|---|---|---|---|---|
| Model | 214.39 | 9 | 23.82 | 76.04 | <0.0001 | Significance |
| *A* | 57.81 | 1 | 57.81 | 184.54 | <0.0001 | Significance |
| *B* | 3.28 | 1 | 3.28 | 10.49 | 0.0230 | Significance |
| *C* | 57.79 | 1 | 57.79 | 184.48 | <0.0001 | Significance |
| *AB* | 4.86 | 1 | 4.86 | 15.50 | 0.0110 | Significance |
| *AC* | 0.1427 | 1 | 0.1427 | 0.4554 | 0.5297 | No significance |
| *BC* | 2.30 | 1 | 2.30 | 7.35 | 0.0422 | Significance |
| $A^2$ | 19.97 | 1 | 19.97 | 63.76 | 0.0005 | Significance |
| $B^2$ | 52.07 | 1 | 52.07 | 166.22 | <0.0001 | Significance |
| $C^2$ | 28.74 | 1 | 28.74 | 91.74 | 0.0002 | Significance |
| Residual | 1.57 | 5 | 0.3133 | | | |
| Lack of fit | 1.33 | 3 | 0.4437 | 3.77 | 0.2167 | No significance |
| Pure error | 0.2353 | 2 | 0.1177 | | | |
| Cor. total | 215.96 | 14 | | | | |

$R^2$ = 0.9927; $R_{Adj}^2$ = 0.9797; $R_{Pred}^2$ = 0.8989.

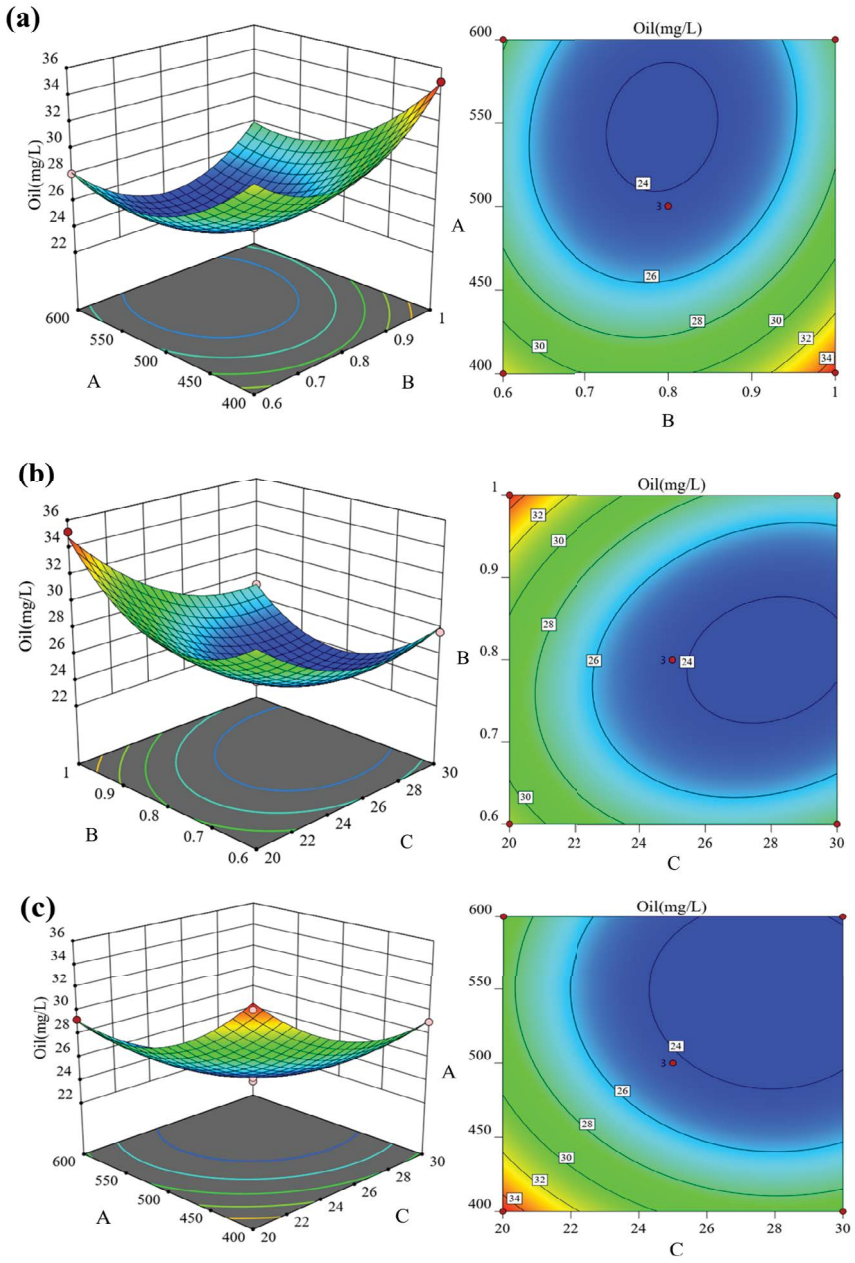


Fig. 4. (a) Interaction of PPA percentage with CQ dosage, (b) interaction of PPA percentage with temperature and (c) interaction of CQ dosage with temperature on oil content in water.

the small decreases of COD and TOC indicate the CQ agent treatment settles in the form of flocs, while the process also removes some dissolved organic matter. Comparing PPA demulsifiers under the same conditions found that the optimized CQ composite agent has a treatment effect comparable to PPA, and the cost of CQ agent is lower. Microscopic pictures of the water samples before and after treatment under optimal conditions were taken using a digital microscope. Before treatment, the water contains more suspended matter and oil droplets, whereas after treatment, the water samples have extremely limited suspended matter, and only a small amount of oil droplets with larger particle size can be seen (Fig. 6).

### *3.6. Demulsification–flocculation mechanism of CQ on TPW wastewater*

#### *3.6.1. Zeta potential analysis*

The mechanism of PPA emulsion breaking was evaluated from the perspective of zeta potential. Fig. 7a reveals the relationship between zeta potential and CQ concentration. The zeta potential of the raw wastewater was −7.152 mV, which is due to the presence of surface-active substances around the oil droplets, which formed a stable double electric layer, resulting in a stronger stabilization of TPW [17,50]. When 100 mg/L of CQ was added, the zeta potential of this system increased to −5.874 mV, which meant some of the

negative surface charges on the oil droplets were neutralized, but the residual unneutralized negative charges still prevented the oil droplets from agglomerating with one another [41]. When the PPA dosage increased to 500 mg/L, the zeta potential of TPW wastewater further increased to −0.721 mV. At this time, a large amount of positively charged CQ was adsorbed on the O/W interface, which neutralized most of the negative surface charge and could attract other dispersed micro-oil droplets by electrostatic force [17,23].

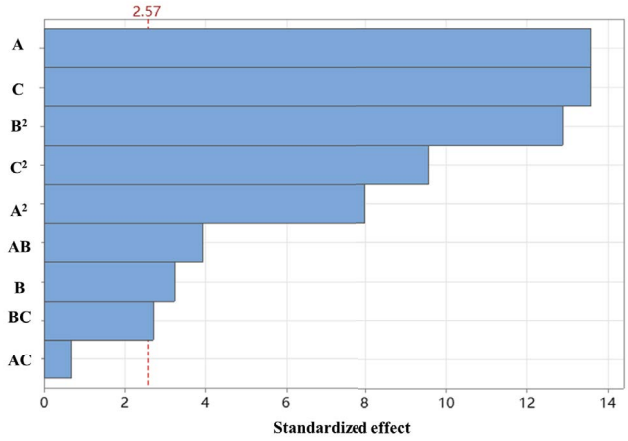


Fig. 5. Standardized Pareto chart for oil content in water.

*3.6.2. IFT analysis*

Static IFT is an important index to evaluate the performance of demulsifier [17]. Different concentrations of CQ demulsification–flocculation were injected into the aqueous phase, and the oil–water IFT was determined by the suspension-drop method. The experimental results in Fig. 7b show CQ can effectively reduce the IFT, and the IFT was significantly reduced from 18.38 to 5.62 mN/m when the dosage was increased from 0 to 500 mg/L, which is because the demulsifier with surface activity can be adsorbed to the oil–water interface, and the adsorption of demulsifier molecules at the oil–water interface increases gradually with the increase of CQ dosage [51,52]. However, when the CQ concentration increased to 600 mg/L, the IFT value almost stopped changing, which means the adsorption of demulsifier molecules at the interface reached saturation; when the CQ dosage was higher than its critical micelle concentration, the demulsifier molecules formed micelles, thus failing to make the IFT decrease further [53].

*3.6.3. Bonding type of CQ with suspended matter and oil droplets*

HCl can form ionic bonds with colloidal particles and hydrogen bonds between urea and colloidal particles, and this property of HCl and urea is used in studies to examine the intermolecular forces of flocculation–precipitation

Table 5
Comparison of several water quality indicators before and after TPW treatment

| Parameter | Before | After | | Change rate | |
|---|---|---|---|---|---|
| | | CQ | PPA | CQ | PPA |
| Oil (mg/L) | 72.63 | 21.26 | 17.02 | 70.73% | 76.57% |
| Total suspended solids (TSS), mg/L | 185.5 | 7.0 | 9.5 | 96.23% | 94.88% |
| Turbidity, NTU | 157.82 | 6.83 | 10.47 | 95.67% | 93.37% |
| Chromaticity, Times | 256 | 8 | 8 | 96.88% | 96.88% |
| Chemical oxygen demand (COD), mg/L | 7,362.02 | 5,127.13 | 5,432.39 | 30.36% | 26.21% |
| Total organic carbon (TOC), mg/L | 1,150.025 | 854.15 | 895.39 | 25.73% | 22.14% |

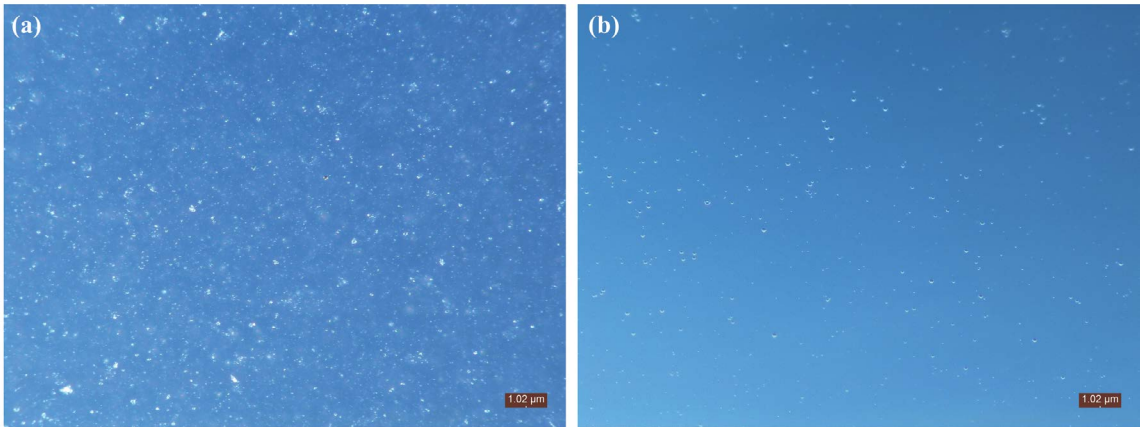


Fig. 6. Digital microscope images of TPW (a) before and (b) after processing.

[54,55]. Therefore, after the flocs settled and 3 mol/L HCl and 5 mol/L urea were added to them (Fig. 8), the flocculation–precipitation was not sensitive to urea but overly sensitive to HCl, and the flocs were almost completely dissolved after the addition of HCl. This outcome indicates the binding between the flocculant and the suspended matter and oil droplets may be by ionic [56].

### 3.6.4. Fractal dimension analysis of flocs

Floc morphology refers to the degree of denseness of the floc produced during flocculation, which was characterized in this paper using the floc fractal dimension ($D_f$) to analyze the degree of denseness and cross-linking of the flocs [57]. The representative flocs after the addition of PPA (Fig. 9a) and CQ (Fig. 9b) to demulsification–flocculation were photographed by an optical microscope with magnified images for the same time. The addition of the compounding modifier improved the floc structure and facilitated the rapid agglomeration of small flocs to become larger. The $D_f$ of PPA flocs and CQ flocs were 1.6659 and 1.8561, respectively, obtained by linear fitting of ln$A$ and ln$P$. The smaller the fractal dimension of flocs is, the higher the porosity and the looser the structure; conversely, the larger the fractal dimension of flocs is, the denser the structure [58,59]. Therefore, the combination of inorganic coagulant PAFC and PPA demulsification can strengthen the net catching and sweeping effect [57].

Based on the above results, the possible demulsification and flocculation mechanism of CQ on TPW can be obtained. After CQ is added to TPW, the block polyether structure of PPA molecules is adsorbed at the oil–water interface to replace the original surfactant. When the oil–water interface is damaged or the strength is reduced, the dispersed emulsified oil merges. At the same time, the structure of polyquaternary ammonium salt makes the surface charge of oil bead produce electric neutralization, which realizes the effect of oil bead coalescence. PAFC is beneficial to improving the floc structure and strengthening the net and sweep to realize the rapid separation of condensate oil and suspended solids from water.

## 4. Conclusion

In this paper, using low-hydrogen-content silicone oil, methyl ether, epoxy ether, and polyquaternary ammonium salt as raw materials, polydendritic polyether–polyquaternary ammonium salt reverse demulsifier was prepared

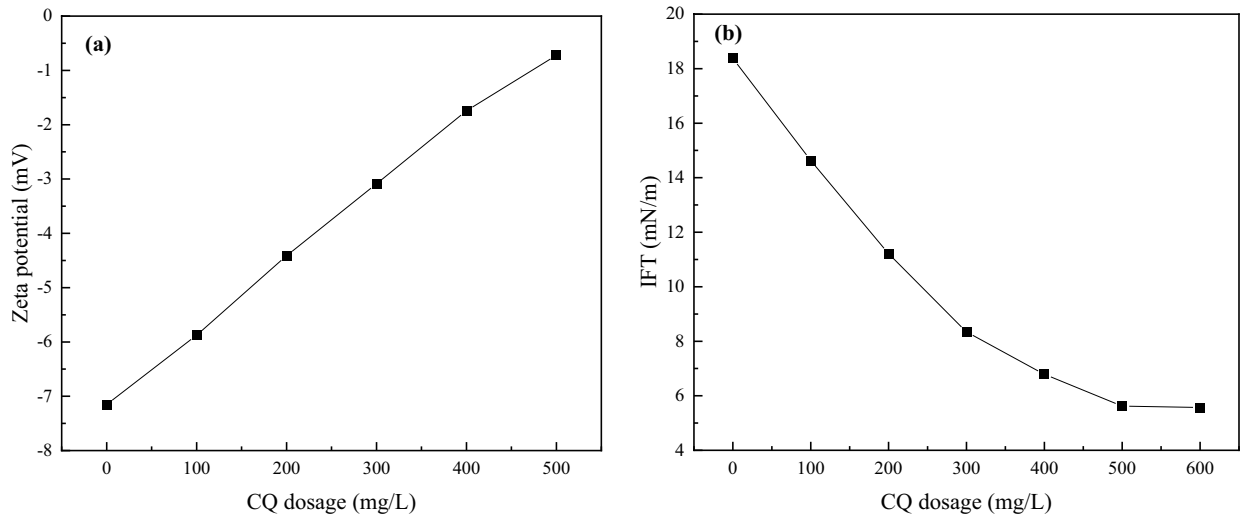


Fig. 7. Effect of CQ dosage on the (a) zeta potential and (b) effect of demulsifier on interfacial tension.

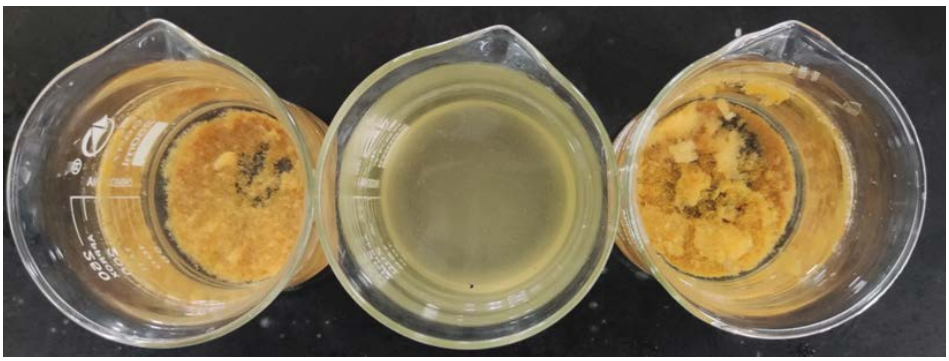

Fig. 8. From left to right, the floc form after adding distilled water, HCl and urea for 10 min.

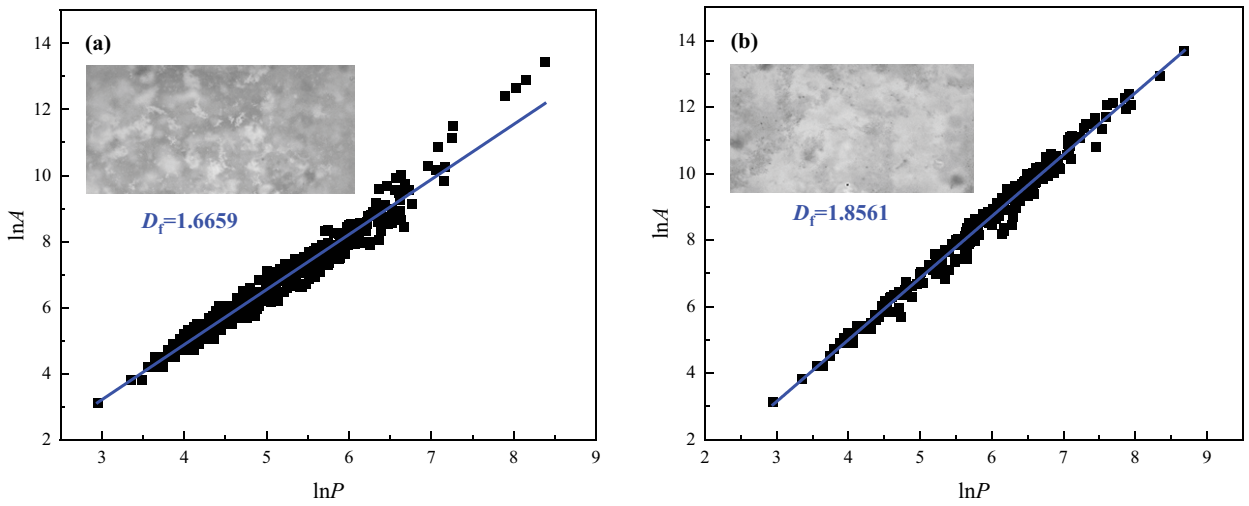


Fig. 9. ln*A*–ln*P* fitting curve of (a) PPA and (b) CQ.

and combined with inorganic coagulant PAFC to obtain a water treatment agent with multifunction of demulsification–flocculation. The characterization of FTIR, XPS, and GPC confirmed PPA contains polyether and polyquaternary ammonium salt structure, and the larger molecular weight is also beneficial to the performance of reverse demulsifier. Under the conditions of CQ concentration of 547 mg/L, settling temperature of 27.9°C and PPA ratio of 71%, the oil content and suspended matter concentration of the TPW in Changqing gas field can be reduced to 21.26 and 7.0 mg/L, respectively, after settling for 30 min, which can meet the technological requirements on site. Response surface analysis showed CQ concentration and settling temperature are the main factors affecting the demulsification–flocculation effect. The positively charged polyquaternary ammonium branch can promote the movement of PPA molecules toward the oil/water interface by electrostatic attraction. Subsequently, due to the strong affinity of the polyether structure for the oil/water boundary mask, PPA molecules replace the original oil/water interface material, so the oil beads and suspended solids coalesce and form a large flocculant to realize the efficient separation of the oil beads, suspended solids, and water. The combination of PAFC can not only reduce the cost but also improve the structure of the floc, which is conducive to the rapid aggregation and enlargement of the small floc.

## Declaration of competing interest

The authors declare that they have no known competing financial interests or personal relationships that could have appeared to influence the work reported in this paper.

## Acknowledgements

The authors of this work wish to gratefully acknowledge the financial support from China National Petroleum Corporation (CNPC) "14th Five-Year Plan" Major Forward-Looking Basic Science and Technology Projects (Research on low-cost oilfield wastewater treatment technology, No. 2021DJ6606).

## Data availability statement

All relevant data are included in the paper or its Supplementary material.

## References

[1] T.L.S. Silva, S. Morales-Torres, S. Castro-Silva, J.L. Figueiredo, A.M.T. Silva, An overview on exploration and environmental impact of unconventional gas sources and treatment options for produced water, J. Environ. Manage., 200 (2017) 511–529.
[2] Y. Li, D. Zhou, W. Wang, T. Jiang, Z. Xue, Development of unconventional gas and technologies adopted in China, Energy Geosci., 1 (2020) 55–68.
[3] X. Tao, M. Gan, Z. Yao, J. Bai, M. Yang, G. Su, L. Zheng, Enhancing the production of tight sandstone gas well through fuzzy-ball fluid temporary plugging with diverting fractures and water cutting after refracturing in one operation, J. Pet. Sci. Eng., 217 (2022) 110883, doi: 10.1016/j.petrol.2022.110883.
[4] X. Tan, C. Jia, J. Liu, G. Liu, R. Zheng, S. Wang, Q. Liu, Gas and water distribution in the tight gas sands of the northwestern daniudi gas field, ordos basin, China: impact of the shale barrier, Fuel, 317 (2022) 122782, doi: 10.1016/j.fuel.2021.122782.
[5] L. Torres, O.P. Yadav, E. Khan, A review on risk assessment techniques for hydraulic fracturing water and produced water management implemented in onshore unconventional oil and gas production, Sci. Total Environ., 539 (2016) 478–493.
[6] C. Guo, H. Chang, B. Liu, Q. He, B. Xiong, M. Kumar, A.L. Zydney, A combined ultrafiltration-reverse osmosis process for external reuse of Weiyuan shale gas flowback and produced water, Environ. Sci. Water Res. Technol., 4 (2018) 942–955.
[7] J. Rosenblum, A.W. Nelson, B. Ruyle, M.K. Schultz, J.N. Ryan, K.G. Linden, Temporal characterization of flowback and produced water quality from a hydraulically fractured oil and gas well, Sci. Total Environ., 596–597 (2017) 369–377.
[8] Y. Lu, Y. Zhang, C. Zhong, J.W. Martin, D.S. Alessi, G.G. Goss, Y. Ren, Y. He, Suspended solids-associated toxicity of hydraulic fracturing flowback and produced water on early life stages of zebrafish (*Danio rerio*), Environ. Pollut., 287 (2021) 117614, doi: 10.1016/j.envpol.2021.117614.
[9] B. Alley, A. Beebe, J. Rodgers, J.W. Castle, Chemical and physical characterization of produced waters from conventional and unconventional fossil fuel resources, Chemosphere, 85 (2011) 74–82.
[10] Y. Li, Y. Wang, Q. Wang, Z. Liu, L. Tang, L. Liang, C. Zhang, Q. Li, N. Xu, J. Sun, W. Shi, Achieving the super gas-wetting alteration by functionalized nano-silica for improving fluid

flowing capacity in gas condensate reservoirs, ACS Appl. Mater. Interfaces, 13 (2021) 10996–11006.
[11] M. Riaz, G.M. Kontogeorgis, E.H. Stenby, W. Yan, T. Haugum, K.O. Christensen, T.V. Lokken, E. Solbraa, Measurement of liquid–liquid equilibria for condensate plus glycol and condensate plus glycol plus water systems, J. Chem. Eng. Data, 56 (2011) 4342–4351.
[12] H. Esmaeili, F. Esmaeilzadeh, D. Mowla, Effect of surfactant on stability and size distribution of gas condensate droplets in water, J. Chem. Eng. Data, 59 (2014) 1461–1467.
[13] C. Wang, Y. Lv, C. Song, D. Zhang, F. Rong, L. He, Separation of emulsified crude oil from produced water by gas flotation: a review, Sci. Total Environ., 845 (2022) 157304, doi: 10.1016/j.scitotenv.2022.157304.
[14] A. Butkovskyi, H. Bruning, S. Kools, H. Rijnaarts, A.P. Van Wezel, Organic pollutants in shale gas flowback and produced waters: identification, potential ecological impact, and implications for treatment strategies, Environ. Sci. Technol., 51 (2017) 4740–4754.
[15] G. Shu, K. Bu, B. Zhao, S. Zheng, Evaluation of newly developed reverse demulsifiers and cationic polyacrylamide flocculants for efficient treatment of oily produced water, Colloids Surf., A, 610 (2021) 125646, doi: 10.1016/j.colsurfa.2020.125646.
[16] C. Shi, L. Zhang, L. Xie, X. Lu, Q. Liu, C.A. Mantilla, F.G.A. van den Berg, H. Zeng, Interaction mechanism of oil-in-water emulsions with asphaltenes determined using droplet probe AFM, Langmuir, 32 (2016) 2302–2310.
[17] H. Sun, Q. Wang, X. Li, X. He, Novel polyether-polyquaternium copolymer as an effective reverse demulsifier for O/W emulsions: demulsification performance and mechanism, Fuel, 263 (2020) 116770, doi: 10.1016/j.fuel.2019.116770.
[18] D. Wang, D. Yang, C. Huang, Y. Huang, D. Yang, H. Zhang, Q. Liu, T. Tang, M. Gamal El-Din, T. Kemppi, B. Perdicakis, H. Zeng, Stabilization mechanism and chemical demulsification of water-in-oil and oil-in-water emulsions in petroleum industry: a review, Fuel, 286 (2021) 119390, doi: 10.1016/j.fuel.2020.119390.
[19] J. Kuang, Y. Mi, Z. Zhang, F. Ye, H. Yuan, W. Liu, X. Jiang, Y. Luo, A hyperbranched poly(amido amine) demulsifier with trimethyl citrate as initial cores and its demulsification performance at ambient temperature, J. Water Process Eng., 38 (2020) 101542, doi: 10.1016/j.jwpe.2020.101542.
[20] J. Zhang, B. Jing, S. Fang, M. Duan, Y. Ma, Synthesis and performances for treating oily wastewater produced from polymer flooding of new demulsifiers based on polyoxyalkylated N,N-dimethylethanolamine, Polym. Adv. Technol., 26 (2015) 190–197.
[21] J. Li, C. Wang, Q. Tang, M. Zhai, Q. Wang, M. Shi, X. Li, Preparation and application of supported demulsifier PPA@$SiO_2$ for oil removal of oil-in-water emulsion, Sep. Sci. Technol., 55 (2020) 2538–2549.
[22] M. Duan, J. He, D. Li, X. Wang, B. Jing, Y. Xiong, S. Fang, Synthesis of a novel copolymer of block polyether macromonomer and diallyldimethylammonium chloride and its reverse demulsification performance, J. Pet. Sci. Eng., 175 (2019) 317–323.
[23] J. Ma, J. Shi, L. Ding, H. Zhang, S. Zhou, Q. Wang, X. Fu, L. Jiang, K. Fu, Removal of emulsified oil from water using hydrophobic modified cationic polyacrylamide flocculants synthesized from low-pressure UV initiation, Sep. Purif. Technol., 197 (2018) 407–417.
[24] J. Zhai, Z.J. Huang, M.H. Rahaman, Y. Li, L.Y. Mei, H.P. Ma, X.B. Hu, H.W. Xiao, Z.Y. Luo, K.P. Wang, Comparison of coagulation pretreatment of produced water from natural gas well by polyaluminium chloride and polyferric sulphate coagulants, Environ. Technol., 38 (2017) 1200–1210.
[25] Y. Sun, C. Zhu, H. Zheng, W. Sun, Y. Xu, X. Xiao, Z. You, C. Liu, Characterization and coagulation behavior of polymeric aluminum ferric silicate for high-concentration oily wastewater treatment, Chem. Eng. Res. Des., 119 (2017) 23–32.
[26] O.S. Amuda, I.A. Amoo, Coagulation/flocculation process and sludge conditioning in beverage industrial wastewater treatment, J. Hazard. Mater., 141 (2007) 778–783.
[27] J.Y. Yang, L. Yan, S.P. Li, X.R. Xu, Treatment of aging oily wastewater by demulsification/flocculation, J. Environ. Sci. Health., Part A Environ. Sci. Eng. Toxic Hazard. Subst. Control, 51 (2016) 798–804.
[28] H. Chang, B. Liu, B. Yang, X. Yang, C. Guo, Q. He, S. Liang, S. Chen, P. Yang, An integrated coagulation-ultrafiltration-nanofiltration process for internal reuse of shale gas flowback and produced water, Sep. Purif. Technol., 211 (2019) 310–321.
[29] M.M. Abdulredha, S.A. Hussain, L.C. Abdullah, Optimization of the demulsification of water in oil emulsion via non-ionic surfactant by the response surface methods, J. Pet. Sci. Eng., 184 (2020) 106463, doi: 10.1016/j.petrol.2019.106463.
[30] K.B. Gregory, R.D. Vidic, D.A. Dzombak, Water management challenges associated with the production of shale gas by hydraulic fracturing, Elements, 7 (2011) 181–186.
[31] X. Zheng, H. Zheng, Y. Zhou, Y. Sun, R. Zhao, Y. Liu, S. Zhang, Enhanced adsorption of Orange G from aqueous solutions by quaternary ammonium group-rich magnetic nanoparticles, Colloids Surf., A, 580 (2019) 123746, doi: 10.1016/j.colsurfa.2019.123746.
[32] Z. Kong, J. Wei, Y. Li, N. Liu, H. Zhang, Y. Zhang, L. Cui, Rapid removal of Cr(VI) ions using quaternary ammonium fibers functioned by 2-(dimethylamino)ethyl methacrylate and modified with 1-bromoalkanes, Chem. Eng. J., 254 (2014) 365–373.
[33] J. Zhuang, N. Rong, X. Wang, C. Chen, Z. Xu, Adsorption of small size microplastics based on cellulose nanofiber aerogel modified by quaternary ammonium salt in water, Sep. Purif. Technol., 293 (2022) 121133, doi: 10.1016/j.seppur.2022.121133.
[34] X. Chen, H. Li, L. Lai, Y. Zhang, Y. Chen, X. Li, B. Liu, H. Wang, Peroxymonosulfate activation using $MnFe_2O_4$ modified biochar for organic pollutants degradation: performance and mechanisms, Sep. Purif. Technol., 308 (2023) 122886, doi: 10.1016/j.seppur.2022.122886.
[35] H. Yuan, F. Ye, G. Ai, G. Zeng, L. Chen, L. Shen, Y. Yang, X. Feng, Z. Zhang, Y. Mi, Preparation of an environmentally friendly demulsifier using waste rice husk as raw materials for oil–water emulsion separation, J. Mol. Liq., 367 (2022) 120497, doi: 10.1016/j.molliq.2022.120497.
[36] A.S. El-Tabei, A.E. El-Tabey, E.A. El-Sharaky, Novel synthesized polymeric surfactants additives based on phenethylamine as an emulsion breaker for water droplet coalescence in naturally Egyptian crude oil emulsion, J. Mol. Liq., 338 (2021) 116779, doi: 10.1016/j.molliq.2021.116779.
[37] N. Nciri, N. Cho, A thorough study on the molecular weight distribution in natural asphalts by gel permeation chromatography (GPC): the case of Trinidad Lake Asphalt and Asphalt Ridge Bitumen, Mater. Today Proc., 5 (2018) 23656–23663.
[38] J. Ma, J. Shi, H. Ding, G. Zhu, K. Fu, X. Fu, Synthesis of cationic polyacrylamide by low-pressure UV initiation for turbidity water flocculation, Chem. Eng. J., 312 (2017) 20–29.
[39] B. Huang, J. Wang, W. Zhang, C. Fu, Y. Wang, X. Liu, Screening and optimization of demulsifiers and flocculants based on ASP flooding-produced water, Processes, 7 (2019) 239, doi: 10.3390/pr7040239.
[40] W.L. Kang, B. Xu, Y.J. Wang, X.H. Shan, Y. Li, Q.C. Liu, Study on stability and treatment of surfactant/polymer flooding wastewater, J. Pet. Sci. Technol., 31 (2013) 880–886.
[41] R. Lyu, Z. Li, C. Liang, C. Zhang, T. Xia, M. Wu, Y. Wang, L. Wang, X. Luo, C. Xu, Acylated carboxymethyl chitosan grafted with MPEG-1900 as a high-efficiency demulsifier for O/W crude oil emulsions, Carbohydr. Polym. Technol. Appl., 2 (2021) 100144, doi: 10.1016/j.carpta.2021.100144.
[42] H. Sun, X. He, Q.Q. Wang, X.B. Li, Demulsification of O/W emulsion using a novel polyether-polyquaternium copolymer: effect of the demulsifier structure and solution environment conditions, Sep. Sci. Technol., 56 (2021) 811–820.
[43] P. Biniaz, M. Farsi, M.R. Rahimpour, Demulsification of water in oil emulsion using ionic liquids: statistical modeling and optimization, Fuel, 184 (2016) 325–333.
[44] J. Mao, G.H. Ni, Y.H. Xu, H. Wang, Z. Li, Z.Y. Wang, Modeling and optimization of mechanical properties of drilling sealing

materials based on response surface method, J. Cleaner Prod., 377 (2022) 134452, doi: 10.1016/j.jclepro.2022.134452.
[45] Y. Zhao, F. Bi, M. Khayet, T. Symonds, X. Wang, Study of seat-to-head vertical vibration transmissibility of commercial vehicle seat system through response surface method modeling and Genetic Algorithm, Appl. Acoust., 203 (2023) 109216, doi: 10.1016/j.apacoust.2023.109216.
[46] Y. Li, Y. Zhou, R. Ni, J. Shang, X. Cheng, Degradation of sulfamethazine sodium salt by peroxymonosulfate activated by biochar supported $CoFe_2S_4$: performance, mechanism and response surface method optimization, J. Environ. Chem. Eng., 10 (2022) 108059, doi: 10.1016/j.jece.2022.108059.
[47] X. Huang, F. Li, Y. Li, X. Meng, X. Yang, B. Sundén, Optimization of melting performance of a heat storage tank under rotation conditions: based on Taguchi design and response surface method, Energy, 271 (2023) 127100, doi: 10.1016/j.energy.2023.127100.
[48] Z.H. Liu, W. Chen, D. Wu, S.X. Wei, M.J. Zhu, Optimized electrocoagulation technology using response surface methodology to control H-2 production and treatment effect of fracturing flowback fluid treated by electrocoagulation, Desal. Water Treat., 262 (2022) 74–88.
[49] D. Li, H. Chen, X. Gao, J. Zhang, Establishment and optimization of partial nitrification/anammox/partial nitrification/anammox (PN/A/PN/A) process based on multi-stage ammonia oxidation: using response surface method as a tool, Bioresour. Technol., 361 (2022) 127722, doi: 10.1016/j.biortech.2022.127722.
[50] M. Fan, C. Nie, H. Du, J. Ni, B. Wang, X. Wang, An insight into the solar demulsification of highly emulsified water produced from oilfields by monitoring the viscosity, zeta potential, particle size and rheology, Colloids Surf., A, 575 (2019) 144–154.
[51] Y. Wang, S. Fang, X. Wang, Y. Wang, Y. Xiong, M. Duan, Synthesis of a novel reverse demulsifier with the characteristics of polyacrylate and polycation and its demulsification performance, J. Appl. Polym. Sci., 138 (2021) 1–11.
[52] R. Zolfaghari, A. Fakhru L-Razi, L.C. Abdullah, S.S.E.H. Elnashaie, A. Pendashteh, Demulsification techniques of water-in-oil and oil-in-water emulsions in petroleum industry, Sep. Purif. Technol., 170 (2016) 377–407.
[53] B. Huang, X.H. Li, W. Zhang, C. Fu, Y. Wang, S.Q. Fu, Study on Demulsification–flocculation mechanism of oil-water emulsion in produced water from alkali/surfactant/polymer flooding, Polymers, 11 (2019) 1–13.
[54] X. Ma, D. Duan, X. Chen, X. Feng, Y. Ma, A polysaccharide-based bioflocculant BP50-2 from banana peel waste: purification, structure and flocculation performance, Int. J. Biol. Macromol., 205 (2022) 604–614.
[55] S. Wang, H. Zhao, D. Qu, L. Yang, L. Zhu, H. Song, H. Liu, Destruction of hydrogen bonding and electrostatic interaction in soy hull polysaccharide: effect on emulsion stability, Food Hydrocolloids, 124 (2022) 107304, doi: 10.1016/j.foodhyd.2021.107304.
[56] Z. Wang, L. Shen, X.L. Zhuang, J.S. Shi, Y.P. Wang, N. He, Y.I. Chang, Flocculation characterization of a bioflocculant from *Bacillus licheniformis*, Ind. Eng. Chem. Res., 54 (2015) 2894–2901.
[57] M. Nadella, R. Sharma, S. Chellam, Fit-for-purpose treatment of produced water with iron and polymeric coagulant for reuse in hydraulic fracturing: temperature effects on aggregation and high-rate sedimentation, Water Res., 170 (2020) 115330, doi: 10.1016/j.watres.2019.115330.
[58] Y.F. Wang, H. Jia, H.W. Zhang, J. Wang, W.J. Liu, Performance of a novel recycling magnetic flocculation membrane filtration process for tetracycline-polluted surface water treatment, Water Sci. Technol., 76 (2017) 490–500.
[59] S.D. Anicio, V.D. Lopes, A.L. de Oliveira, PSD and fractal dimension for flocculation with different parameters and ferric chloride, aluminium polychloride and aluminium sulfate as coagulants, J. Water Process Eng., 43 (2021) 102180, doi: 10.1016/j.jwpe.2021.102180.